

FEW-ELECTRON LIQUID AND SOLID PHASES IN ARTIFICIAL MOLECULES AT HIGH MAGNETIC FIELD

MASSIMO RONTANI (rontani@unimore.it), GUIDO GOLDONI (goldoni@unimore.it) and ELISA MOLINARI
INFN National Research Center on nanoStructures and bioSystems at Surfaces (S³) and Dipartimento di Fisica, Università degli Studi di Modena e Reggio Emilia, Via Campi 213/A, 41100 Modena, Italy

Abstract. Coupled semiconductor quantum dots form artificial molecules where relevant energy scales controlling the interacting ground state can be easily tuned. By applying an external magnetic field it is possible to drive the system from a weak to a strong correlation regime where eventually electrons localize in space in an ordered manner reminiscent of the two-dimensional Wigner crystal. We explore the phase diagram of such “Wigner molecules” analyzing the angular correlation function obtained by the Configuration Interaction solution of the full interacting Hamiltonian. Focus is on the role of tunneling in stabilizing different ground states.

1. Introduction

Semiconductor quantum dots (QDs) are zero-dimensional systems where a few electrons, typically $1 < N < 100$, are spatially confined and the energy spectrum is completely discrete [1]. Carriers can be injected one by one to the system in single-electron transport [2] or capacitance [3] experiments, based on the *Coulomb blockade* [4] phenomenon, and the energy required to add one electron can be measured if the electrostatic screening is poor and the thermal smearing is low. Measurements of such “electron affinities” [2] have revealed a shell structure for the correlated electron system and fine corrections to the energy due to exchange interaction (Hund’s rule): therefore QDs are often regarded as *artificial atoms* [5, 6]. In Fig. 1 we compare the relevant parameters of natural and artificial atoms: note that for the latter the typical energy spacing is of the order of a few meV, less than the thermal energy at experimentally reachable temperatures [1]. *Artificial molecules* can be built by coupling two QDs together in a controlled way [7, 8]: this additional degree of freedom enriches the physics of natural

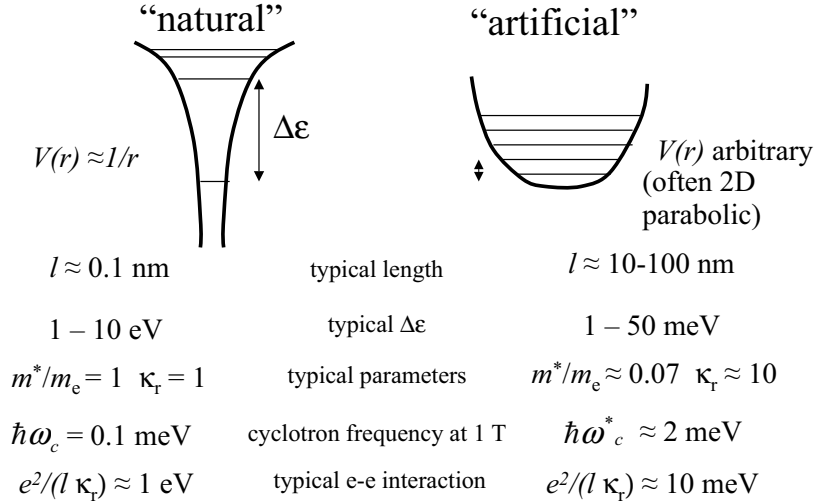


Figure 1. Comparison between the typical parameters and energy scales of “natural” and “artificial” atoms. m^* and κ_r are the effective mass and the static dielectric constant of the host semiconductor, respectively. The (effective) cyclotron frequency ω_c (ω_c^*) is defined as eB/mc (eB/m^*c), with B applied magnetic field.

molecules, since for the latter the inter-nuclear coupling is almost fixed by the balance between nuclear repulsion and electrostatic attraction mediated by valence electrons, while in the former the stability of the electron system is externally imposed.

Current focus on QDs stems from their technological potentialities as optoelectronic devices (single-electron transistors [4], lasers [9], micro-heaters and micro-refrigerators based on thermoelectric effects [10]) as well as from several proposals of quantum information processing schemes in a solid-state environment [11, 12]. Here however we are more interested in basic physical principles and we look at QDs as a laboratory to explore the fundamentals of few-body strongly interacting systems.

The plan of the paper is the following: Section 2 is a primer on electron states in QDs. We show which energy scales can be artificially tailored and their effect on the interacting ground states. After, we specialize to the case of the artificial molecule in very high magnetic field as a paradigm of the strong correlation regime (Sec. 3).

2. Manipulating the energy spectrum

The critical issue of artificial atoms and molecules is that almost all relevant energy scales can be controlled by means of fabrication and/or tuning of experimental parameters such as voltages or magnetic fields and made of comparable size. [1, 8, 13]. This is at difference with natural systems, where, for example, the dominant energy scale is provided by the ionic potential attracting the valence electrons, while the weaker electron-electron interactions can be treated reasonably well by mean field methods. Moreover, the orbital and spin coupling with an external magnetic field is very small (cfr. Fig. 1). The ground states are therefore determined by the successive filling of the empty lowest-energy hydrogen-like orbitals, according to the *Aufbau* theory. The open-shell configurations are well described by Hund's rules, which can be explained as the effect of the Coulomb term in the interacting Hamiltonian.

In QDs the confining potential $V(\mathbf{r})$ is much weaker, being provided by the electrostatic environment. Here effective parameters, such as renormalized electron mass and static dielectric constant of the host semiconductor determine the kinetic energy, the strength of the Coulomb interaction, and the coupling with the field (see Fig. 1). The overall effect is that there is no dominant energy scale (Fig. 1), making the problem of determining the electronic ground state much more difficult.

In many of the experimental realizations of artificial atoms, the system can be regarded as quasi two dimensional [1]: since the confinement along the growth direction z is much tighter than in the $x-y$ plane, the z degree of freedom is frozen as far as low-energy states are concerned. In the effective mass and envelope function approximation, the confinement potential $V(\mathbf{r})$ can be decoupled as

$$V(\mathbf{r}) = V(\boldsymbol{\rho}) + V(z), \quad (1)$$

with $\boldsymbol{\rho} \equiv (x, y)$. Lowest-energy states are very well described by a two dimensional harmonic oscillator potential

$$V(\boldsymbol{\rho}) = m^* \omega_0^2 \rho^2 / 2, \quad (2)$$

where m^* is the effective mass of the host semiconductor. Adequacy of Eq. (2) has been demonstrated both by theoretical calculations [14] and far infra-red spectroscopy [1]; in addition, it is the lowest order approximation in the Taylor expansion of the weak electrostatic potential.

The single-electron Hamiltonian $H_0(\mathbf{r}, s_z)$ is

$$H_0(\mathbf{r}, s_z) = (-i\hbar\nabla + |e|\mathbf{A}/c)^2 / 2m^* + V(\mathbf{r}) + g^* \mu_B B s_z, \quad (3)$$

where we included a magnetic field parallel to the z axis $\mathbf{B} = B\hat{z}$ which couples with both the spin degree of freedom, $s_z = \pm 1/2$, and the orbital

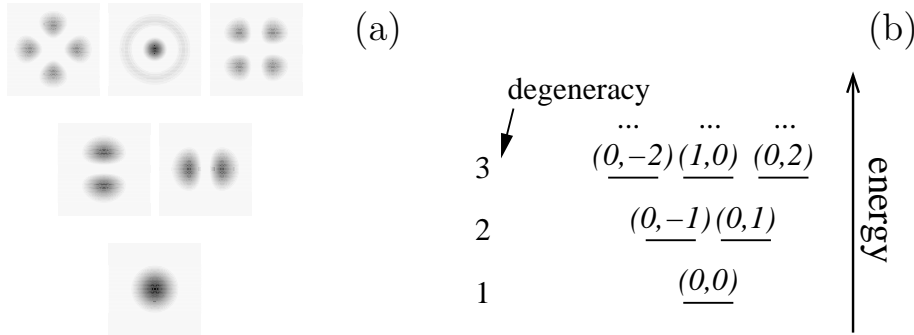


Figure 2. Two dimensional harmonic trap: The energy structure at zero field. (a) Contour plot in the $x - y$ plane of the probability density of the first lowest-energy single-particle orbitals. (b) Energy shell structure. The couple of numbers (n, m) refer to the radial and azimuthal single-particle quantum numbers, respectively.

motion via the vector potential $\mathbf{A} = \mathbf{B} \times \boldsymbol{\varrho}/2$. Note that, since the Bohr magneton of the *free* electron μ_B enters (3), the spin part is usually negligible with respect to the orbital part (g^* is the effective gyromagnetic factor).

Because of the decoupling (1), we can write the eigenfunctions of the orbital part of the Hamiltonian (3) as $\psi_{nm}(\mathbf{r}) = \varphi_{nm}(\boldsymbol{\varrho}) \chi(z)$, where $\chi(z)$ is the ground state for the motion along z and $\varphi_{nm}(\boldsymbol{\varrho})$ are the eigenstates of the 2D harmonic oscillator (Fock-Darwin levels, Fig. 2 and 3). The eigenvalues ε_{nm} are given by

$$\varepsilon_{nm} = \hbar\Omega(2n + |m| + 1) - \hbar\omega_c^*m/2, \quad (4)$$

where n ($n = 0, 1, 2, \dots$) and m ($m = 0, \pm 1, \pm 2, \dots$) are the radial and azimuthal quantum numbers, respectively, ω_c^* is the cyclotron frequency ($\omega_c^* = eB/m^*c$), and $\Omega = (\omega_0^2 + \omega_c^{*2}/4)^{1/2}$ [1]. When $B = 0$ ($\omega_c^* = 0$) the Fock-Darwin spectrum shows a characteristic shell structure (Fig. 2): the level degeneracy linearly increases with the shell number [Fig. 2(b)], and the energy spacing between neighboring shells is constant (see Fig. 2).

A magnetic field parallel to the growth direction splits the degeneracies of the states (Fig. 3) and “squeezes” the orbitals, as it appears from the expression of the characteristic length $\ell = (\hbar/m^*\Omega)^{1/2}$, corresponding to the average value of ϱ on the ground state φ_{00} : the stronger the field, the smaller the radius of the wavefunction. At intermediate fields ($\omega_c \sim \omega_0$) the energy levels may increase or decrease as a function of the field, depending whether the azimuthal quantum number m is negative or positive; at large fields, however, all levels tend to the 2D highly degenerate Landau levels.

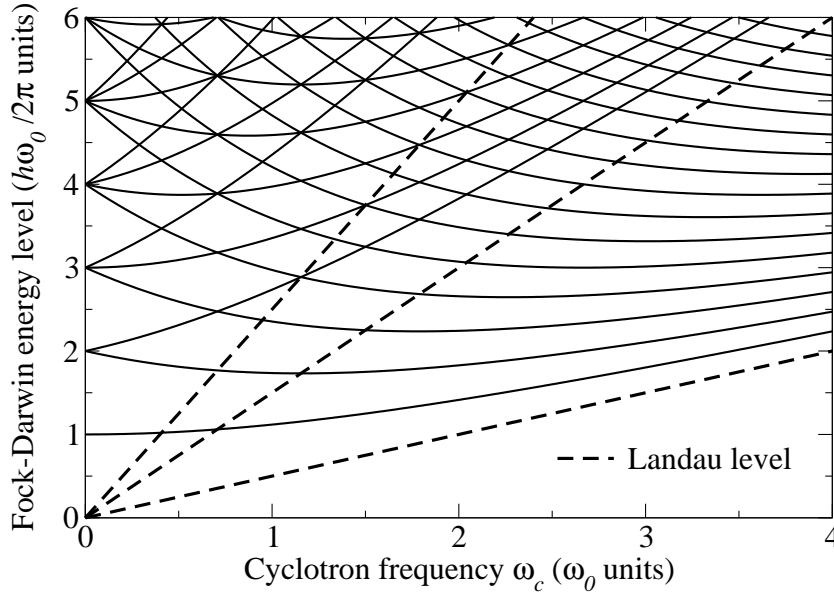


Figure 3. Two dimensional harmonic trap: The single-particle Fock-Darwin levels in a magnetic field B . The energies are given in units of $\hbar\omega_0$. The field dependence is contained in the cyclotron frequency $\omega_c^* = eB/m^*c$. The first three lowest-energy Landau levels are also depicted.

The latter can be obtained by letting $\omega_c^*/\omega_0 \rightarrow \infty$ in Eq. (4). Accordingly, at large fields only positive m states are occupied ($n = 0$). In this limit, the energy separation $\Delta\varepsilon$ between levels differing on $|\Delta m| = 1$ becomes $\Delta\varepsilon \approx \hbar\omega_0^2/\omega_c^*$, which is $\propto 1/B$.

Additional flexibility in controlling the energy spectrum is given by the possibility to grow QDs coupled by quantum mechanical tunnelling. A typical “vertical” device is sketched in Fig. 4(a) (see ref. [15] for an experimental realization). In this case, the carrier dynamics is not strictly 2D anymore, as two levels $\chi_i(z)$ [symmetric ($i = S$) and anti-symmetric ($i = AS$) for a “homonuclear” molecule, see Fig. 4(c)] enter the relevant energy range. Correspondingly, the single particle spectrum comprises two sets of Fock-Darwin states at small [Fig. 4(d)] or high [Fig. 4(e)] magnetic fields. The energy separation between S and AS states is $2t$, t being the tunneling energy which can be controlled, e.g., by varying the width d or the height V_0 of the inter-dot potential barrier while growing the sample [Fig. 4(c)].

When we consider the Coulomb interaction between carriers, no exact solutions are available except very special cases for $N = 2$ [16]. The

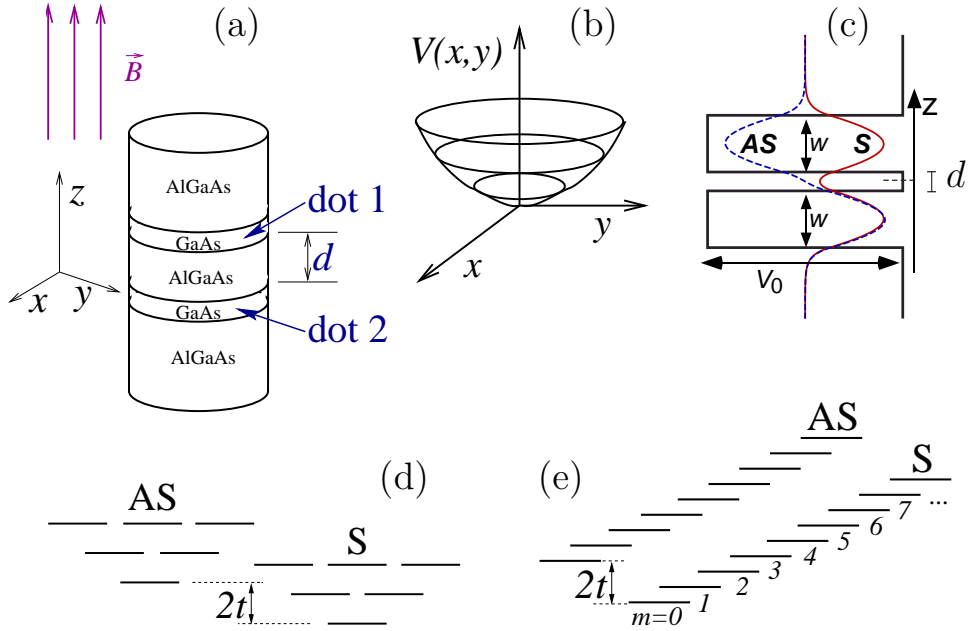


Figure 4. Model of the vertical artificial molecule. (a) Sketch of the model device we consider. (b) In-plane single-particle confinement potential. (c) Confinement potential along the z -axis. V_0 and d are respectively the height and the width of the inter-dot potential barrier, while w is the thickness of each of the two dots. (d) The symmetric (S) and antisymmetric (AS) sets of Fock-Darwin levels at zero field. t is the tunneling energy. (e) The S and AS sets of Fock-Darwin levels in a high magnetic field. Only the first lowest-energy states with $n = 0$ and $m > 0$ are depicted.

interacting Hamiltonian

$$\mathcal{H} = \sum_{i=1}^N H_0(\mathbf{r}_i, s_{zi}) + \frac{1}{2} \sum_{i \neq j} \frac{e^2}{\kappa_r |\mathbf{r}_i - \mathbf{r}_j|}, \quad (5)$$

with κ_r static dielectric constant, must be solved numerically. Dramatic alterations of the few-body energy spectrum and wavefunctions appear, depending on the relative ratio of the magnitudes of the one- and two-body terms in \mathcal{H} .

If the single-electron term H_0 prevails, the system basically behaves as a non-interacting system, or, better, as a Fermi liquid with corrections due to the residual part of the interaction. This is the regime where the periodic table of artificial atoms has been observed [2]. If instead the Coulomb term dominates, electrons undergo a transition to a qualitatively new state where they orderly arrange themselves in space in such a manner to minimize the

electrostatic energy [1, 5, 17]. In this few-body strongly correlated regime, which is reminiscent of the Wigner crystal phases in extended systems [18], the physics turns out to be classical. Asymptotically, all operators become commutative and all spin configurations tend to perfect degeneracy (except possibly the Zeeman splitting).

The Wigner regime can be artificially driven in two ways. One possibility is fabrication of QDs with weak enough lateral confinement that the average electron density n is extremely small: since the 2D one-electron term in Eq. (5) goes like n while the two-body term like $n^{1/2}$, in the dilute limit the former becomes negligible with respect to the latter [17]. Another possibility is to apply a magnetic field strong enough that the energy separation $\Delta\varepsilon$ becomes small compared to the typical Coulomb energy (equivalently, $\ell \ll n^{-1/2}$): again, the interaction term of \mathcal{H} controls the low-energy physics. We focus on this case in Sec. 3.

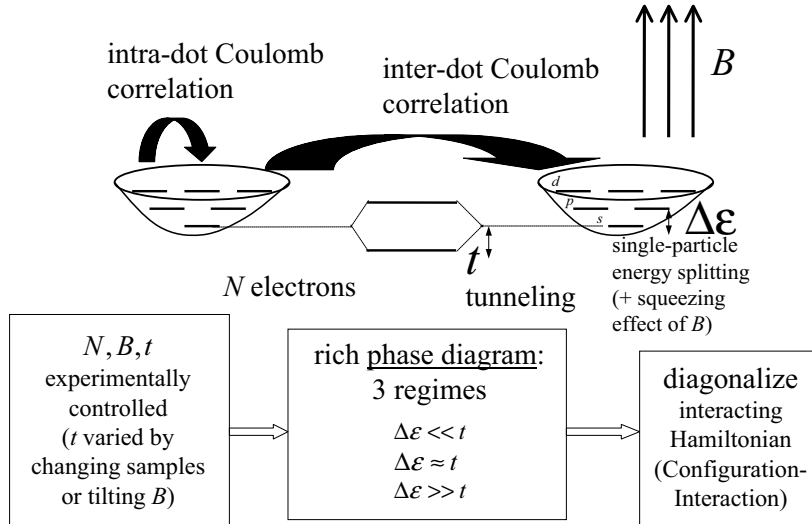


Figure 5. Artificial molecules: The relevant energy scales controlling the few-electron interacting ground state. Many of these energies can be artificially tuned together with the number of electrons N .

Figure 5 summarizes the relevant energy scales for a coupled QD system and how they can be tailored. Both single particle energies and tunneling can be independently tuned by device engineering or, more practically, by external magnetic field intensity and direction. The “degree” of correlation of the system can be similarly controlled, as well as N .

3. Structural transitions in Wigner molecules

We now discuss the ground state of N electrons in coupled QDs in a high magnetic field B , i.e., such that single-QD correlation functions show strong localization [8, 19]. We present results for $N = 6$ [19]. The system with $N < 6$ exhibits a similar physics. We can identify three regimes corresponding to different electron arrangements: (I) At small d , tunneling dominates and the system behaves as a unique coherent system. (II) As d is increased, all energy scales become comparable. (III) When eventually tunneling is suppressed, only the ratio between intra- and inter-dot interaction is the relevant parameter for the now well separated QDs.

To analyze the ground state of the artificial molecule in the different regimes, we show in Fig. 6 the pair correlation function $P(\boldsymbol{\rho}, z; \boldsymbol{\rho}_0, z_0) = \sum_{i \neq j} \langle \delta(\boldsymbol{\rho} - \boldsymbol{\rho}_i) \delta(z - z_i) \delta(\boldsymbol{\rho}_0 - \boldsymbol{\rho}_j) \delta(z_0 - z_j) \rangle / N(N-1)$ (the average is on the ground state) [8, 19]. Since we are interested in the strong localization regime, we expect that spin texture does not alter the essential physics, therefore we assume that electrons are spin polarized [20]. Figure 6 shows $P(\boldsymbol{\rho}, z; \boldsymbol{\rho}_0, z_0)$ along a circle in the same dot (solid line) or in the opposite dot (dashed line) with respect to the position of a reference electron, taken at the maximum of its charge density, $(\boldsymbol{\rho}_0, z_0)$. The right column shows the electron arrangement in the QDs as inferred by the maxima of $P(\boldsymbol{\rho}, z; \boldsymbol{\rho}_0, z_0)$.

At small d the whole system is coherent, i.e., it behaves as a unique QD. The electrons, delocalized over the dots, arrange at the vertices and the center of a regular pentagon (Phase I). At intermediate values of the tunnelling energy electrons sit at the vertices of a regular hexagon. Contrary to the previous case peaks in the upper and lower dots have different heights (Phase II). Finally, when d is sufficiently large, the structure evolves into two isolated dots coupled only via Coulomb interaction. Accordingly, three electrons in each dot sit at the vertices of two equilateral triangles rotated by 60 degrees (Phase III).

It is important to note from Fig. 6 that Phase I and III are strongly localized phases, where quantum fluctuations play a minor role, and electron configurations are basically determined by Coulomb interactions; accordingly, they have completely classical counterparts [21]. On the contrary, in Phase II tunneling fluctuations prevents electron from localizing and therefore the configuration has a “liquid” character. Such phase cannot be explained in term of Coulomb interactions solely and, in fact, the exagonal arrangement shown in Fig. 6 is classically unstable.

This example shows that in artificial molecules at high B one can drive qualitative changes in the ground state of the interacting electrons that are clearly precursors of quantum phase transitions in the infinite system

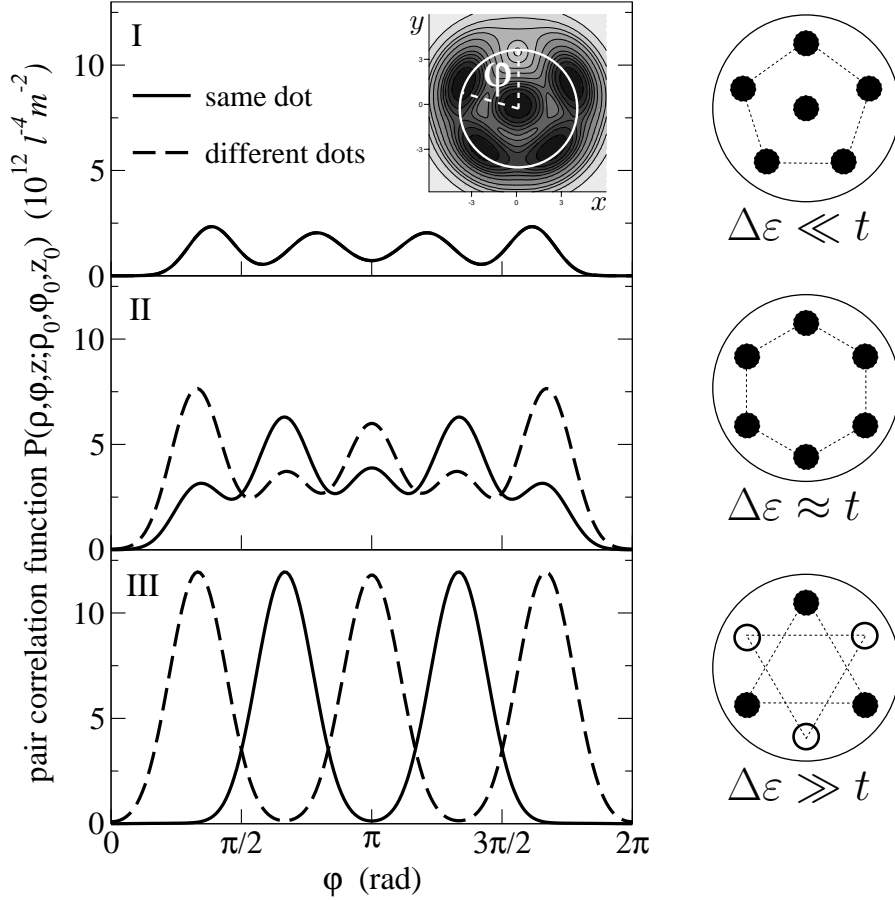


Figure 6. The three phases of the Wigner molecule as the critical ratio $\Delta\varepsilon/t$ is changed. Here we numerically solve the Hamiltonian of Eq. (5) by means of the Configuration Interaction method, namely we expand the few-body wavefunction as a linear combination of Slater determinants made by filling with N electrons the Fock-Darwin orbitals. We consider only levels with $m > 0$ and $n = 0$. Further details in ref. [19]. B is fixed (25 T) and we assume as parameters (see text and caption of Fig. 4) $\hbar\omega_0=3.70$ meV, $w=12$ nm, $V_0=250$ meV, $m^*=0.067m_e$, $\kappa_r=12.4$, $g^*=-0.44$ as typical values of realistic devices [15]. The three phases correspond to $d=2, 4.6, 8$ nm, respectively.

[22]. While the observation of such transitions in the bulk is very difficult, QDs seem to constitute ideal systems to explore in the laboratory the fundamentals of electron correlation. For example, it is conceivable that inelastic light scattering spectroscopy is able to probe the different roto-vibrational “normal modes” of the three phases, thus allowing for their experimental detection. See ref. [19] for further details.

Acknowledgements

This work was supported by INFN (SSQI), by MIUR (FIRB Quantum Phases of Ultra-Low Electron Density Semiconductor Heterostructures), by MAE (Progetto di Particolare Rilevanza “Controllo di stati di carica e spin in punti quantici”), and by the EC (SQID).

References

1. For reviews see: L. P. Kouwenhoven *et al.*, in *Mesoscopic electron transport*, edited by L. L. Sohn, L. P. Kouwenhoven, and G. Schoen (Kluwer, Dordrecht, 1997), p. 105; L. Jacak, P. Hawrylak, and A. Wójs, *Quantum dots* (Springer, Berlin, 1998); D. Bimberg *et al.*, *Quantum dot heterostructures* (Wiley, Chichester, 1998); T. Chakraborty, *Quantum dots: A survey of the properties of artificial atoms* (North-Holland, Amsterdam, 1999); L. P. Kouwenhoven, D. G. Austing, and S. Tarucha, *Rep. Prog. Phys.* **64**, 701 (2001).
2. S. Tarucha *et al.*, *Phys. Rev. Lett.* **77**, 3613 (1996).
3. R. C. Ashoori, *Nature* **379**, 413 (1996).
4. H. Grabert and M. H. Devoret, *Single charge tunneling: Coulomb blockade phenomena in nanostructures*, NATO ASI series B: physics **294** (Plenum, New York, 1992).
5. P. Maksym and T. Chakraborty, *Phys. Rev. Lett.* **64**, 108 (1990).
6. M. A. Kastner, *Phys. Today* **46**, 24 (January 1993).
7. L. P. Kouwenhoven, *Science* **268**, 1440 (1995).
8. For a review see M. Rontani *et al.*, *Solid State Commun.* **119**, 309 (2001).
9. Y. Arakawa and H. Sakaki, *Appl. Phys. Lett.* **40**, 939 (1982); N. Kirstaedter *et al.*, *Electron. Lett.* **30**, 1416 (1994).
10. H. L. Edwards *et al.*, *Phys. Rev. B* **52**, 5714 (1995).
11. G. Burkard, D. Loss, and D. P. DiVincenzo, *Phys. Rev. B* **59**, 2070 (1999).
12. F. Troiani, U. Hohenester, and E. Molinari, *Phys. Rev. B* **62**, R2263 (2000); E. Biolatti *et al.*, *Phys. Rev. Lett.* **85**, 5647 (2000).
13. M. A. Reed, *Scientific American* **268**, 98 (1993).
14. A. Kumar, S. E. Laux, and F. Stern, *Phys. Rev. B* **42**, 5166 (1990).
15. D. G. Austing *et al.*, *Physica B* **249-251**, 206 (1998).
16. M. Taut, *Phys. Rev. A* **48**, 3561 (1993).
17. G. W. Bryant, *Phys. Rev. Lett.* **59**, 1140 (1987).
18. E. Wigner, *Phys. Rev.* **46**, 1002 (1934); A. Ishiara, *Solid State Phys.* **42**, 271 (1989); R. Côté in *Microscopic theory of semiconductors*, edited by S. W. Koch (World Scientific, London, 1995), p. 315.
19. M. Rontani *et al.*, *Europhys. Lett.* **58**, 555 (2002).
20. At smaller B spin plays an important role; see e.g. L. Martín-Moreno, L. Brey, and C. Tejedor, *Phys. Rev. B* **62**, R10633 (2000).
21. B. Partoens, V. A. Schweigert, and F. M. Peeters, *Phys. Rev. Lett.* **79**, 3990 (1997).
22. Here we mean phase transitions driven by continuously changing some parameter of the interacting Hamiltonian at vanishingly low temperatures: see S. Sachdev, *Quantum phase transitions*, (Cambridge University Press, 1999).